AIAA'88

AIAA-88-2944
Linear Theory of Active Control of Pressure Oscillations in Combustion Chambers

V. Yang, A. Sinha, and Y. T. Fung
The Pennsylvania State University
University Park, PA 16802

AIAA/ASME/SAE/ASEE 24th JOINT PROPULSION CONFERENCE

JULY 11-13, 1988/Boston, Massachusetts

Linear Theory of Active Control of Pressure Oscillations in Combustion Chambers

Vigor Yang*, Alok Sinha*, and Yung-Teh Fung**
Department of Mechanical Engineering
The Pennsylvania State University
University Park, PA 16802

ABSTRACT

Active control of longitudinal pressure oscillations in combustion chambers has been studied theoretically using a digital state-feedback control technique. The formulation is based on a generalized wave equation which accommodates various influences on combustion, mean flow, unsteady motions, and contol actions. After a procedure equivalent to the Galerkin method, a system of ordinary differential equation governing the amplitude of each oscillatory mode is derived, serving as a basis for the controller design. The control actions is provided by a finite number of point acutators, with the instantaneous chamber conditions monitored by a few sensors. Several important control aspects such as sampling period, locations of sensors and controllers, controllability and observability have been investigated. As a specific example, the case involving two controlled and two residual (uncontrolled) modes is studied. The control and observation spillover phenomena due to the residual modes are clearly demonstrated.

I. Introduction

The desire to advance propulsion technology has led to efforts to control and optimize various operation characteristics of combustion systems. Principal among them is the moderation or control of pressure oscillations in combustion chambers, which are generally known as combustion instabilities. Heat release by combustion is the source of energy sustaining such oscillations. There seems little doubt that the most intense motions owe their existence to the mutual coupling between unsteady combustion response and periodic flow oscillations. As a result, the oscillations appear as the motions of a self-excited system. The ensuing structure vibrations and thrust variations may significantly comprise the overall system performance.

Many attempts have been made to overcome combustion instability problems or to prevent their occurrence. The efforts usually fall into two categories: (1) making changes in the system designs so that the coupling between the combustion response and unsteady wave motions can be minimized; and (2) making changes in the dynamic energy losses so that they exceed the energy gains from the combustion response. Although these methods have demonstrated their effectiveness in certain situations, a number of fundamental problems still remain unresolved. First, most of existing techniques are static in nature and based on passive means. The instability suppression systems operate only for a narrow frequency range and do not respond effectively to the spatial and temporal variations of flow conditions. Second, no unified general theories have been constructed as to the optimization of control systems. The entire system was developed primarily on a trial-and-error basis. The experience gained from one system may not be directly applicable to other systems. Third, perhaps more important, for many practical systems there is even no passive means available for controlling instabilities.

While traditional passive control techniques need improvements and further optimization, a new technology based on active instability control (AIC) offers radically new solutions, particularly in the regime where passive control techniques are ineffective, impractical, too costly, or have reached their design limits. The AIC methods incorporate modern control theories and offer capabilities of estimating the instantaneous flow conditions, calculating the optimum control feedback coefficients, and exerting control actions on the flow fields. Figure 1 shows the schematic of the proposed system. The important physical variables in the combustor are monitored by appropriate sensors at representative positions. The measured signals are then filtered and processed by a microprocessor in which the optimal control gains are calculated instantaneously according to a predescribed model. Finally, the control inputs are activated to modify the flow conditions. If designed properly, it may attenuate any undesired oscillations within a few cycles. Recent work[1-4] on the control of thermo-acoustic oscillations has clearly demonstrated the advantages the AIC technique.

The purpose of this paper is to provide a theoretical framework for studying the active control of combustion instabilities. In what follows, a general analysis of unsteady motions in a combustion chamber is first given, followed by a comprehensive discussion of the controller design. As a specific example, the case involving a finite number of controlled and residual modes are addressed in detail.

II. Formulation

The model described here can be applied to broad classes of problems encountered in practical systems. To concentrate on the construction of active control algorithms, we restrict the following discussion to the special case of longitudinal oscillations in a uniform chamber. The formulation extends the previous analyses for nonlinear combustion instabilities[5,6] and

---

* Assistant Professor, Member AIAA

** Graduate Student

accommodates actively controlled external forcing. In brief, the conservation equations for a two-phase mixture of gas and particulates are first written in the following form.

$$\frac{\partial \rho}{\partial t} + \vec{v} \cdot \nabla \rho = - \rho \nabla \cdot \vec{v} + W \qquad (2.2)$$

$$\rho \frac{\partial \vec{v}}{\partial t} + \rho \vec{v} \cdot \nabla \vec{v} = - \nabla p + \vec{F} \qquad (2.2)$$

$$\frac{\partial p}{\partial t} + \gamma p \nabla \cdot \vec{v} = - \vec{v} \cdot \nabla p + P \qquad (2.3)$$

The function W represents the mass conversion rate of condensed phases to gas per unit volume, F is the force of interaction between the gas and condensed phases, and P is the sum of the heat release associated with chemical reaction and the energy transfer between two phases.

A wave equation governing the unsteady motions is then derived with decomposition of the dependent variables into mean and time-dependent quantities. To simplify matters here we shall ignore variations in the mean pressure, temperature, and density, but the mean flow velocity is both non-zero and non-uniform. Thus,

$$\rho = \bar{\rho} + \rho'(t,\vec{r}) \qquad (2.4)a$$

$$\vec{v} = \vec{v}\,(\vec{r}) + \vec{v}'(t,\vec{r}) \qquad (2.4)b$$

$$p = \bar{p} + p'(t,\vec{r}) \qquad (2.4)c$$

Since combustion instabilities manifest themselves by the presence of pressure oscillations and the pressure signals can be directly measured and processed at sufficiently frequencies, the wave equation can be most conveniently written in terms of pressure. Now substitute (2.4) in (2.1) - (2.3), collect coefficients of like powers, and rearrange the results to obtain the following wave equations:

$$\frac{\partial^2 p'}{\partial t^2} - \bar{a}^2 \nabla^2 p' = h + h_c \qquad (2.5)$$

subject to the boundary condition

$$\vec{n} \cdot \nabla p' = - f - f_c \qquad (2.6)$$

where the subscript c represents the control inputs. The functions h and f contain all linear and nonlinear influences of acoustic motions, mean flow, and combustion, under conditions with no external forcing. Their explicit expressions are given in Ref. 6.

In this work, the control force h_c consists of M point actuators for supplying acoustic pressure excitations at appropriate positions

$$h_c(\vec{r},t) = \sum_{k=1}^{M} \xi_k(t)\, b_k(\vec{r}) \qquad (2.7)$$

The forcing amplitudes are $\xi_k(t)$, and the influence functions $b_k(\vec{r})$ are represented by the Dirac delta functions $\delta(\vec{r} - \vec{r}_k)$ to simplify the analysis. The pressure field and its time rate of change are monitored by P point sensors. Thus the output signal has the following form.

$$y_j = c_j\, p'(\vec{r}_j,t) + d_j \frac{\partial p'}{\partial t}(\vec{r}_j,t), \qquad j = 1,2, \ldots, P \qquad (2.8)$$

where c_j and d_j are fixed real numbers.

For many practical combustion chambers, the most dominant unsteady motions have structures and frequencies closely related to those of classical acoustic modes of the chamber. The solution of the wave equation (2.5) can therefore be approximated by a synthesis of the normal modes, but with unknown time-varying amplitudes,

$$p'(\vec{r},t) = \bar{p} \sum_{n=1}^{L} \eta_n(t)\, \psi_n(\vec{r}) \qquad (2.9)$$

where ψ_n is the normal mode function satisfying

$$\nabla^2 \psi_n + k_n^2 \psi_n = o \qquad (2.10)$$

$$\vec{n} \cdot \nabla \psi_n = o$$

For longitudinal pressure oscillations in a uniform chamber,

$$\psi_n = \cos \frac{n\pi}{L_c} z \qquad (2.11)$$

where L_c is the chamber length. In theory, the system requires an infinite number of modes ($L \to \infty$) to completely describe its behavior. However, in practice, the unsteady motions can be represented with good fidelity by a truncated modal expansion of (2.9), in which L may be large but still finite. This approximation is well justified by the fact that the high frequency oscillations can be efficiently damped out by viscous dissipation and may not exist physically. In addition, the actuators and sensors can not excite or response to the very high frequency modes.

After substitution of (2.9) in (2.5) and with the aid of the spatial averaging, a set of ordinary differential equations is obtained for the amplitude of each mode.

$$\ddot{\eta}_n + \omega_n^2 \eta_n + \sum_{j=1}^{L} (D_{nj}\dot{\eta}_j + E_{nj}\eta_j) + F_N(\eta_1,\eta_2 \ldots \dot{\eta}_1,\dot{\eta}_2,..) = a_n \omega_n(t) + b_n u_n(t), \quad n = 0,1,2,\ldots L \qquad (2.12)$$

where $\omega_n(t)$ is the random noise, D_{nj} and E_{nj} are linear coefficients associated with the growth rate and frequency shift, respectively, and F_N represents the nonlinear processes. The control input can be written as

$$u_n(t) = \frac{\bar{a}^2}{p\, E_n^2} \sum_{k=1}^{M} \xi_k(t)\, \psi_n(\vec{r}_k) \qquad (2.13)$$

in which E_n^2 denotes the norm of the mode shape.

Similarly, the sensor output equation has the following form.

$$y_j = c_j \bar{p} \sum_{n=1}^{L} \eta_n(t)\, \psi_n(\vec{r}_j) + d_j \bar{p} \sum_{n=1}^{L} \dot{\eta}_n(t)\, \psi_n(\vec{r}_j)$$

$$j = 1,2,\ldots,P \qquad (2.14)$$

The system (2.12)-(2.14) can be described as stochastic, nonlinear, and many dimensional. As a first attempt, we treat only the deterministic and linear behavior of the system, i.e., $\omega_N(t) = o$ and $F_N = o$. The problems involving nonlinearity and stochastic processes will be dealt with in subsequent work.

III. Construction of State-Feedback Control

In this section, a digital control system based on the state-feedback technique is developed. The goal is to optimize the control input $u_n(t)$ such that the amplitude of pressure oscillation $\eta_n(t)$ can be controlled within a prespecified level as $t \to \infty$. In according with (2.9), the oscillatory behavior of the combustor chamber is described by L modes. Realistically, however, it may not be practical to control all these modes because the actuators and sensors can not excite or respond to the high frequency modes. In addition, the on-board computer limitations and model errors would restrict the control to a few critical modes. If only the first N modes are controlled with $N < L$, the state variables (defined here as pressure oscillations and their time derivatives) can be partitioned into a controlled and and uncontrolled (residual) part.

$$X = X_N + X_R \qquad (3.1)$$

where

$$X_R^T = [\eta_{N+1}, \dot{\eta}_{N+1}, \ldots, \eta_L, \dot{\eta}_L]$$

The subscripts N and R represents the controlled and residual modes, respectively. Thus, from (2.10) and (2.12), the state-space and output equations can be written in the following vector form.

$$\begin{aligned} \dot{X}_N(t) &= A_N X_N(t) + B_N u(t) \\ \dot{X}_R(t) &= A_R X_N(t) + B_R u(t) \\ y(t) &= C_N X_N(t) + C_R X_R(t) \end{aligned} \qquad (3.2)$$

where A_N and A_R are the system parameter matrices associated with the controlled and residual modes, respectively, B_N and B_R are the control input matrices, and C_N and C_R the sensor output matrices. The control input and sensor output vectors are defined as follows

$$u^T(t) = [\xi_1(t), \xi_2(t), \ldots, \xi_M(t)] \qquad (3.3)$$

$$y^T(t) = [y_1(t), y_2(t), \ldots y_P(t)] \qquad (3.4)$$

To simplify the problem, it is proposed to use a zero-order-hold (ZOH) technique to convert a digital to a continuous signal, or vice versa. Therefore, the state-space and output equations in discrete time can be written as

$$X(k+1) = F X(k) + G U(k) \qquad (3.5)$$

$$y(k) = C X(k) \qquad (3.6)$$

where

$$F = e^{AT_S} \qquad (3.7)a$$

$$G = \left(\int_0^{T_S} e^{A\tau} d\tau\right) B \qquad (3.7)b$$

and T_S is the sampling period. The functions $X(k)$ denotes the state at the time of kT_S. Note that for a given system, the matrices F and G are determined mainly by the actuator positions and the sampling period. For the computation of the elements of F and G, the efficient algorithm described in Ref. 7 has been used.

Controller Design

The active controller has two major functions:

1) accommodation of a state estimator which receives the sensor measurements $y(t)$ and calculates an estimate $\hat{X}_N(t)$ of the state $X_N(t)$; and
2) determination of the feedback control gain such that $\eta_n(k) \to o$ as $k \to \infty$.

Since the states $X(t)$ are in general not directly available, a Luenberger observer[8] s employed to estimate them in accordance with the control input and the sensor output. Then the state estimate $X_N(t)$ is multiplied by a constant control gains and fedback to the plant to ensure the system stability (see Fig. 2).

Since the presence of residual modes in the output may destabilize a closed-loop system which is based on the estimated states,[9] it is proposed to filter them out. Let the filtered output be

$$y_f(k) = C_N X_N(k) \qquad (3.8)$$

The estimator therefore has the form

$$\hat{X}_N(k+1) = F \hat{X}_N(k) + G u(k) + L (y_f(k) - C_N \hat{X}_N(k)) \qquad (3.9)$$

where L is the estimator gain matrix, and the superscript $\hat{}$ denotes the estimated state. Because the estimator does not have the capability to determine the initial state, for convenience, $\hat{X}_N(0)$ is usually set to be zero. The state feedback law is of the following form:

$$u(k) = - K \hat{X}_N(k) \qquad (3.10)$$

where K is the control feedback gain matrix. Now substitute (3.8) and (3.10) in (3.9) to obtain the expression for the estimator error $e_N(t)$.

$$e_N(k+1) = (F - LC_N)\, e_N(k) \qquad (3.11)$$

with

$$e_N(k) \equiv X_N(k) - \hat{X}_N(k) \qquad (3.12)$$

Equation (3.11) indicates that the decay of estimator error $e_N(k)$ is governed by the eigenvalues of the matrix $F - L C_N$. It is obvious that the $F - L C_N$ should be located inside the unit circle of the z-plane. For desired locations of these eigenvalues, one can always first determine the estimator gain L, provided that the state is observable. This is related to the conditions for the system observability, which requires the following matrix $\mathcal{O}$ be nonsingular.

$$\mathcal{O} \equiv \begin{pmatrix} C \\ CF \\ CF^2 \\ \cdot \\ \cdot \\ \cdot \\ CF^{N-1} \end{pmatrix} \tag{3.13}$$

Even though only the estimated states are fedback, the control gains K can be computed by assuming that the states are known. This is the well-known separation principle. When the states are exactly known, the closed-loop system matrix becomes $F - GK$, as shown by Eq. (3.5). Therefore, to ensure the system stability, the control gain matrix K must be carefully determined such that the eigenvalues of $F - GK$ are located inside the unit circle in the z-plane, as well as that the condition for controllabilityis fulfilled. This usually requires a nonsingularity of the controllability matrix defined as follows

$$\mathcal{C} = [F \; FG \; F^2G \; \ldots \; F^{N-1}G] \tag{3.14}$$

Determination of Controller and Estimator Gain Matrices, K and L

Now let the open-loop characteristic equation be described as

$$\det(zI - F) = z^{2N} + a_1 z^{2N-1} + \ldots + a_{2N} \tag{3.15}$$

The coefficients $a_1, \ldots, a_{2N}$ can be determined by the knowledge of the eigenvalues of F. For a closed-loop system, the system and estimator characteristic equations can be written respectively as

$$\det(zI - F + GK) = z^{2N} + \alpha_1 z^{2N-1} + \ldots + \alpha_{2N} \tag{3.16a}$$

$$\det(zI - F + LC) = z^{2N} + \beta_1 z^{2N-1} + \ldots + \beta_{2N} \tag{3.16b}$$

The controller and estimator gain matrices (K and L) are then evaluated according to the following expressions.[7]

$$K = (\alpha - a) P^{-1} \mathcal{C}^{-1} \tag{3.17a}$$

$$L = \mathcal{O}^{-1} (P^T)^{-1} (\beta - a) \tag{3.17b}$$

where

$$(\alpha - a) = [\alpha_1 - a_1, \; \alpha_2 - a_2, \; \ldots \; \alpha_{2N} - a_{2N}] \tag{3.18a}$$

$$(\alpha - a) = [\beta_1 - a_1, \; \beta_2 - a_2 \; \ldots \; \beta_{2N} - a_{2N}] \tag{3.18b}$$

and P is a upper triangular Toeplitz matrix.

Note that the coefficients in the polynomials (3.16)a and (3.16)b can be determined by the desired eigenvalues of the matrices $(F - GK)$ and $(F - LC)$, respectively.

Locations of Actuator and Sensor

The locations of the actuators must be carefully selected because they influence the controllability matrices. If these matrices are singular, the actuator can not control all the states. To enhance the system controllability, the coefficients of the input should be as large as possible for the controlled modes. On the other hand, the input signal which drives the controlled states to zero will also excite the residual modes. The phenomenon is commonly known as control spillover and should be minimized as much as possible. Hence, the coefficients of the input in (3.14) should be as small as possible for the uncontrolled (residual) modes.

In order to increase the system controllability and reduce the control spillover, the actuator location z_a should be chosen to minimize the following objective function.

$$J = a \sum_{n=1}^{N} [1 - \psi_n (z_a)]^2 + b \sum_{n=N+1}^{L} [\psi_n (z_a)]^2 \tag{3.19}$$

For longitudinal pressure oscillations, $\psi_i(z_a)$ is closely related to the normal mode shape and can be defined as

$$\psi_i (z_a) = \cos \frac{n\pi}{L_c} z_a \tag{3.20}$$

The objective function J is plotted as a function of the actuator location z_a, as shown in Fig. 3. It is concluded that the best actuator location is $z_a = L_c/6.5$.

Equation (3.18) also suggests that the minimization of (3.18) would lead to a reduction in the observation spillover. The sensor is therefore also located at $L_c/6.5$. In other words, the sensor and the actuator are calculated.

IV. Discussion of Results

The theoretical formulation and the active control algorithm described in the previous sections can be applied effectively to suppress pressure oscillations in a uniform chamber. To illustrate the digital controller design, two controlled and two residual modes of longitudinal oscillations are considered. Their system linear coefficients D_{ij} and E_{ij} in (2.21) are given below.

D_{ij}	j=1	2	3	4
i=1	-0.01	0	0	0
2	0	0.1	0	0
3	0	0	0.5	0
4	0	0	0	5.0

E_{ij}	j=1	2	3	4
i=1	0.02	0	0	0
2	0	-0.02	0	0
3	0	0	0.02	0
4	0	0	0	0.02

The first mode is unstable and the second mode is stable. The linear coupling terms, D_{ij} and E_{ij} with $i \neq j$, are ignored for simplicity, but can be included straightforwardly. In addition, only one sensor is employed to estimate the states and one actuator is used to provide the stabilizing control input.

The control procedure contains the following four steps. First, the actuator and sensor location is selected to be at z = Lc/ 6.5, to maximize the effects of actuator on the controlled modes and to minimize the influences on the residual modes. Second, a suitable value of sampling time is chosen to provide a good degree of system observability and controllability. Third, the observer and controller pole locations are carefully selected. In this work, the closed-loop system pole locations are Z = 0.991, 0.990, 0.940, and 0.930, respectively. The observer poles are about three times faster than the system poles to ensure a good overall system performance. These pole locations are Z = 0.9732, 0.9703, 0.8044, and 0.8306, respectively.

Figure 4 shows the calculated results for the controlled modes. The sampling period T_S is 0.04. The controller functions quite effectively and can eliminate undesired oscillations within a few cycles. Figure 5 shows the time traces of the residual oscillations. The controll spillover phenomenon is clearly seen. Small oscillations begin to grow after the controller is activated, then decay when the system becomes stable. The estimator errors e_N are also calculated, giving the results shown in Fig. 6. The observer is capable of estimating the states closely, except for the short initial transient period.

One of the fundamental issues associated with the active control system is the tradeoff between the energy of unsteady motions and the energy required to eliminate oscillations. To see this, the input pressure at the actuator location is also calculated. Figure 7 indicates that the system really needs a small amount of energy in the initial stage to control the oscillations. Further investigation of the energy aspect of the problem is currently underway and will be reported in subsequent work.

V. Conclusion

A linear theory has been developed to study the active control of combustion instabilities in combustion chamber. The control action is provided by M point actuators, with the instantaneous chamber conditions monitored by P point sensors. The effects of sampling period and locations of sensors and actuators on the system controllability and observability are examined. As an example, the case involving a finite number of longitudinal modes of oscillations are considered. Results clearly demonstrate the control and observation spillover phenomenon due to the residual (uncontrolled) modes. The work represents the first in a series of attempts to investigate theoretically various techniques for the active control of combustion instabilities.

REFERENCES

1. Sreenivasan, K. R., Raghu, S. and Chu, B. T., "The Control of Pressure Oscillations in Combustion and Fluid Dynamical Systems," AIAA Paper 85-05440, 1985.

2. Bloxsidge, G. J., Bowling, A. P., Hooper, N., and Langhorne, P. J., "Active Control of an Acoustically Drive Combustion Instability," Journal of Theoretical and Applied Mechanics, Vol. 6, 1987, pp. 161-175.

3. Bloxsidge, G. J., Dowling, A. P., Hooper, N., and Langhorne, P. J., "Active Control of Reheat Buzz," AIAA Paper 87-0433, 1987.

4. Poinsot, T., Bourienne, F., Esposito, E., Candel, S., Lang, W., "Suppression of Combustion Instabilities by Active Control," AIAA Paper 87-1876, 1987.

5. Culick, F. E. C., "Nonlinear Behavior of Acoustic Waves in Combustion Chambers," Acta Astronautica, Vol. 3, 1976, pp. 715-756.

6. Culick, F. E. C. and Yang, V. "Theories of Nonsteady Combustion in a Solid Propellant Rocket and Predictions of Rocket Motor Stability," (Invited Chapter) To Appear in Nonsteady Burning and Combustion Stability of Solid Propellants, Progress in Astronautics and Aeronautics, ed. by L. DeLuca and M. Summerfield.

7. Kailath, T., Linear Systems, Prentice-Hall, Inc., 1980.

8. Luenberger, D., "An Introduction to Observers." IEEE Trans. on Automatic Control, Vol. AC-16, pp. 596-602, 1971.

9. Balas, M. J., "Feedback Control of Flexible Systems," IEEE Trans. on Automatic Control, Vol. AC-23, No. 4, 673-679, 1978.

10. Franklin, G. F. and Powell, J. D., Digital Control of Dynamic Systems, Addison-Weseley, Ince., 1980.

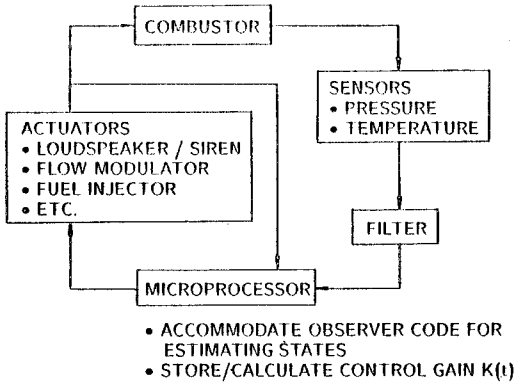

Fig. 1. Schematic Diagram of Active Control of Combustion Instabilities

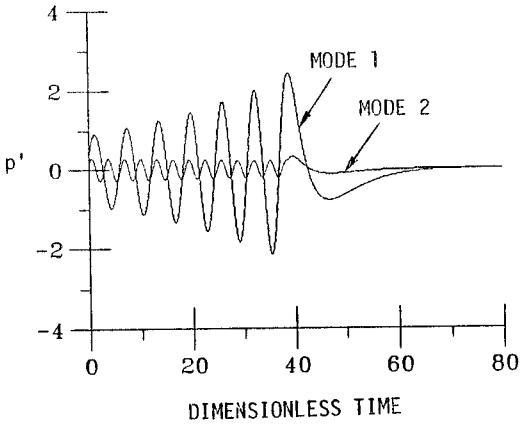

Fig. 4. Time Traces of Controlled Modes of Oscillations; $\omega_1 = 1$, $\omega_2 = 2$

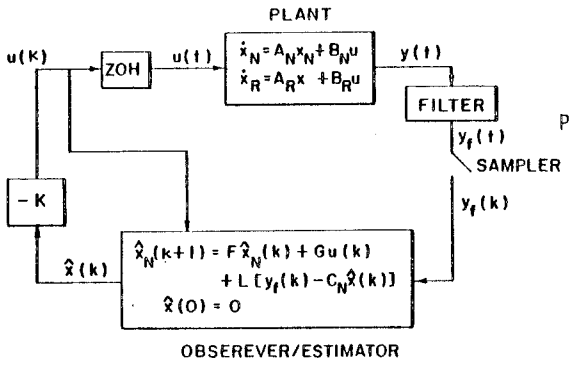

Fig. 2. Structure of the Digital Control System

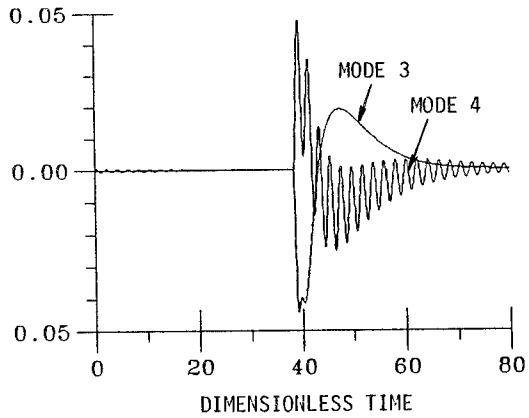

Fig. 5. Time Tracer of Residual Modes of Oscillations; $\omega_3 = 3$, $\omega_4 = 4$

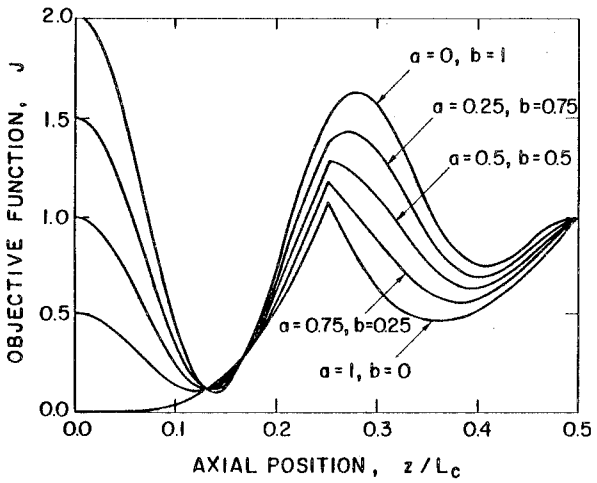

Fig. 3. Objective Function for Selection of Actuator and Sensor Locations; Two Controlled and Two Residual Modes

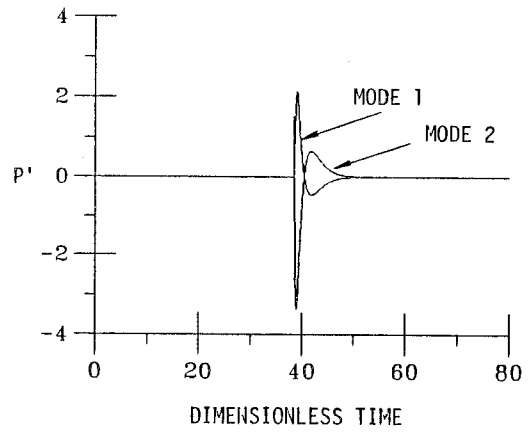

Fig. 6. Time Trace of the Estimator Error

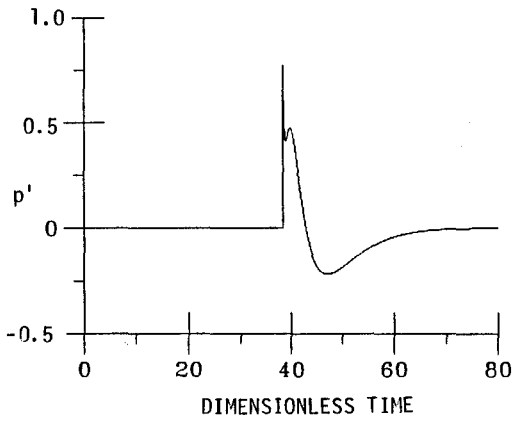

Fig. 7. Time Trace of the Control Input